JOURNAL OF NANO- AND ELECTRONIC PHYSICS
Vol. **10** No 2, 02031(6pp) (2018)

ЖУРНАЛ НАНО- ТА ЕЛЕКТРОННОЇ ФІЗИКИ
Том **10** № 2, 02031(6cc) (2018)

Studies on Cu and TiO_2 Water-based Nanofluids: A Comparative Approach in Laminar Flow

Y. Khelili[1,*], A. Allali[1,†], R. Bouakkaz[2]

[1] *Aircraft Laboratory, Department of Mechanical Engineering, Univ. Blida 1, Algeria*
[2] *Department of Mechanical Engineering, Univ. Constantine 1, Algeria*

(Received 08 November 2017; published online 29 April 2018)

In this paper, a numerical simulation has been performed to study the fluid fllow and heat transfer around a circular cylinder utilizing Cu and TiO_2 water-based nanofluids over low Reynolds numbers. Here, the Reynolds number is varied within the range of 1 to 40 and the volume fraction of nanoparticles (φ) is varied within the range of $0 < \varphi < 0.05$. Two-dimensional and steady mass continuity, momentum, and energy equations have been discretized using finite volume method. SIMPLE algorithm has been applied for solving the pressure linked equations. The effect of volume fraction of nanoparticles on fluid flow and heat transfer were investigated numerically. It was found that at a given Reynolds number, the Nusselt number, drag coefficient, re-circulation length, and pressure coefficient increases by increasing the volume fraction of nanoparticles.

Keywords: Nanofluid steady flow, Finite volume, Circular cylinder, Reynolds number, Volume fraction.

DOI: 10.21272/jnep.10(2).02031 PACS numbers: 47.15.G –, 47.15. – x

1. INTRODUCTION

Forced convection heat transfer is an important phenomenon in engineering and industry with widespread application in diverse field, suchas, microelectronics, transportation, nuclear power plants, cooling of microchips in computers, and heat exchangers and other industrial system in various sectors. Recently, a new class of heat transfer fluids, called nanofluids, has been developed by suspending nanocrystalline particles in fluids. Nanofluids are thought to be the next-generation heat transfer fluids, and they offer exciting possibilities due to their enhanced heat transfer performance compared to ordinary fluids.

Since the initiative experimental work on the thermal conductivity in nanofluids by Masuda a substantial number of investigations have been carried out to report excellent thermal conductivity and heat transfer characteristics associated with nanofluids. These include Choi, Yu, Maxwell, Das et al., Xuan et al., Eastman et al., Lee et al., Hester et al. and many other scientists and researchers. A recent development is that nanoparticles can be dispersed in conventional heat transfer fluids such as water, glycol, or oil to produce a new class of high efficiency heat exchange media. Valipour and Zare Ghadi [1]. Their results showed that as the solid volume fraction increases, the magnitude of minimum velocity in the wake region and recirculation length increases but separation angle decreases. The momentum and forced convection heat transfer for a laminar and steady free stream flow of nanofluids past an isolated square cylinder have been studied numerically by V E-Farooji et al. [2]

M. S. Valipour et al. [3] investigated a numerical simulation has been performed to study the fluid flow and heat transfer around a square cylinder utilizing AL_2O_3-H_2O nanofluid over low Reynolds numbers. The Reynolds number is varied within the range of 1 to 40 and the volume fraction of nanoparticles (φ) is varied within the range of $0 < \varphi < 0.05$. Soares et al. [4] used the stream function-vorticity approach to solve the momentum and thermal energy equations to obtain the detailed velocity and temperature fields for three values of Reynolds number (5, 20 and 40) as functions of the power law index and Prandtl number (1-100). Ogawa et al. [5], experimentally investigated the viscoelastic effects on the forced convection mass transfer in polymer solutions around a sphere and a circular cylinder in the Reynolds number range $1 < \mathrm{Re} < 200$, the main thrust of these studies was to develop drag correlations. Srinivas et al. [6] studied numerically effet of convection from an isothermally heated circular cylinder for wide range of power index ($0.2 \le n \le 1.8$), Reynods number ($1 \le \mathrm{Re} \le 40$) and Prandtl number ($1 \le \mathrm{Pr} \le 100$). They found that average Nusselt number shows a contrary dependence on power-law index but a positive dependence on Re and Ri.

Another numerical study on fluid flow and heat transfer around a solid circular cylinder utilizing nanofluid was done by Sarkar et al. [7] investigated numerically. They presented the effects of Re, Ri and φ (thus m and n values of shear-thinning power-law nanofluids) on mixed convective heat transfer from non-Newtonian nanofluids to circular cylinders in a vertical flow configuration. A.S. Dalkilic [8] has reported critical information on theoretical, experimental and numerical work related to forced convection heat transfer of nanofluids.

The present investigation had been motivated by increased interest and research in potential improvements in heat transfer characteristics using nanofluids, typically for flow characterized by low Reynolds number. Effort has been made to study effect of nanoparticles on the transport phenomena around a circular cylinder maintained at constant temperature.

* khliliyacine1@gmail.com
† r.bouakkaz@gmail.com

2. PROBLEM STATEMENT AND MATHEMATICAL FORMULATION

Consider the two-dimensional, laminar flow of an incompressible Newtonian fluid with a uniform inlet velocity U_∞ and temperature, T_∞ across an infinitely long (in z-direction) circular. To convert the physical problem into a computational equivalent, a circular cylinder of diameter D is placed concentrically in a circular domain of diameter D_∞ as shown in Fig. 1. The radius of the enveloping circular domain is chosen to be sufficiently large in order to minimize the boundary effects. The surface of the solid cylinder is maintained at a constant wall temperature, T_w. The thermo-physical properties (viscosity, density, heat capacity and thermal conductivity) of the streaming liquid are assumed to be independent of the temperature and the viscous dissipation effects in the energy equation are neglected in this study.

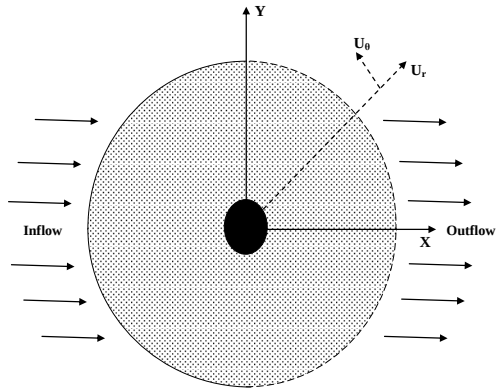

Fig. 1 – Schematics of the unconfined flow around a circular cylinder

Starting from minimum Re of 10. In order to keep the flow physics in essentially the steady two dimensional regime, maximum Reynolds number in this study is restricted to 40.

Figure 1 shows the computational domain used in this investigation. The corresponding distance between the top and bottom boundaries is 40D.

2.1 Governing Equations

The governing partial differential equations; Navier stokes and energy equations in dimensionless form for two dimensional incompressible flow (with constant thermo-physical property) are given by (1)-(4).

Continuity Equation:

$$\frac{\partial U_r}{\partial r} + \frac{U_r}{r} + \frac{1}{r}\frac{\partial U_\theta}{\partial \theta} = 0 \tag{1}$$

r – Momentum Equation:

$$(\vec{V}.\vec{\nabla})U_r - \frac{{U_\theta}^2}{r} = -\frac{\rho_f}{\rho_{nf}}\frac{\partial P}{\partial r} + \frac{2}{v_f Re}\frac{\mu_{nf}}{\rho_{nf}}\left(\nabla^2 U_r - \frac{2}{r^2}\frac{\partial U_\theta}{\partial \theta} - \frac{U_r}{r^2}\right) \tag{2}$$

θ – Momentum Equation:

$$(\vec{V}.\vec{\nabla})U_\theta + \frac{U_r U_\theta}{r^*} = -\frac{\rho_f}{\rho_{nf} r}\frac{\partial P}{\partial \theta} + \frac{2}{v_f Re}\frac{\mu_{nf}}{\rho_{nf}}\left(\nabla^2 U_\theta + \frac{2}{r^2}\frac{\partial U_r}{\partial \theta} - \frac{U_\theta}{r^2}\right) \tag{3}$$

Energy Equation:

$$(\vec{V}.\vec{\nabla})T = \frac{k_f}{k_{nf}}\frac{(\rho C_p)_{nf}}{(\rho C_p)_f}\frac{2}{RePr} \times (\nabla^2 T) \tag{4}$$

With $\nabla^2 = \frac{\partial^2}{\partial r^{*2}} + \frac{1}{r^*}\frac{\partial}{\partial r^*} + \frac{1}{r^{*2}}\frac{\partial^2}{\partial \theta^{*2}} + \frac{\partial^2}{\partial z^{*2}}$

The fluid properties are described by the density ρ, viscosity μ, specific heat C_p and thermal conductivity k.

2.2 Thermal Properties of Nanofluids

Density: The density of nanofluids at different volume concentrations and temperatures are obtained from the literature. The nanofluids density calculated with the equation from Pak and Cho (1998).

$$\rho_{nf} = (1\text{-}\varphi)\rho_{f+}\varphi\rho_p \tag{5}$$

For typical nanofluids with nano particles of volume fraction less than 1 %, a variation of less than 5 % in the fluid density is expected.

Specific heat: The specific heat of a nanofluid can be calculated by using energy balance as:

$$(\rho C_p)_{nf} = (1\text{-}\varphi)(\rho C_p)_f + \varphi(\rho C_p)_p \tag{6}$$

Where, φ is the nano particle volume fraction and is given as:

$$\varphi = \frac{Volume\ of\ nanoparticles}{Total\ volume\ of\ solution}$$

The Eqs. (5) and (6) were introduced by *Buongiorno* (2006).

The Brownian motion has a significant impact on the effective thermal conductivity. Koo and Kleinstreuer (2005) proposed that the effective thermal conductivity is composed of the particle's conventional static part and a Brownian motion part. This 2-component thermal conductivity model takes into account the effects of particle size, particle volume fraction, and temperature.

$$k_{nf} = k_{static} + k_{Brownian}$$

$$\frac{k_{static}}{k_f} = \frac{k_p + 2k_f\text{-}2(k_f\text{-}k_p)\varphi}{k_p + 2k_f + (k_f + k_p)\varphi}$$

$$k_{Brownian} = 5 \times 10^4 \beta\varphi\rho_f C_{p.f}\sqrt{\frac{kT}{2\rho_p d_p}}f(T,\varphi)$$

$$\frac{k_{static}}{k_f} = \frac{k_p + 2k_f\text{-}2(k_f\text{-}k_p)\varphi}{k_p + 2k_f + (k_f + k_p)\varphi}$$

$$k_{Brownian} = 5 \times 10^4 \beta\varphi\rho_f C_{p.f}\sqrt{\frac{kT}{2\rho_p d_p}}f(T,\varphi)$$

Where $k = 1.3809 \times 10^{-23}$ J/k is the Boltzmann

constant, and β is given as:

$$\beta = 8.4407(100\varphi)^{-1.07304}$$

and $f(T,\varphi)$ is given as:

$$f(T,\varphi) = (2.8217\times10^{-2}\varphi + 3.917\times10^{-3})\left(\frac{T}{T_0}\right)$$

$$(-3.0669\times10^{-2}\varphi - 3.91123\times10^{-3})$$

The effective dynamic viscosity for the nano-fluid could be calculated by the following equations (Corcione 2010):

$$\mu_{nf} = \frac{\mu_f}{\left(1 - 34.87\left(d_p/d_f\right)^{-0.3}\times\varphi^{1.03}\right)}$$

$$d_f = \left(\frac{6M}{N\pi\rho_{f0}}\right)^{1/3}$$

Where d_p and d_f represented the mean diameter of the nanoparticles and equivalent diameter of a base fluid molecule, respectively; M represented the molecular weight; N represented the Avogadro number = 6.022 9 10^{23} mol^{-1}; and ρ_{f0} is the density of the base fluid found at Temperature = 293 K.

3. RESULTS AND DISCUSSION

The governing equations mentioned in previous section are discretized based on finite volume approach. The governing equations are integrated over a staggered grid arrangement. A pressure correction based iterative algorithm, SIMPLE is used to solve the pressure linked equations. Central difference scheme is used to discretize the diffusion terms whereas a combination of upwind and central difference is adopted for discretizing the convection terms.

The thermos-physical properties of the fluid and the nanoparticle, copper, are listed in Table 1

Table 1 – Thermophysical properties of nanoparticle and base fluid

	k ($W.m^{-1}.K^{-1}$)	ρ ($Kg.m^{-3}$)	$\mu\ 10^{-3}$ ($Kg.m^{-1}.s^{-1}$)	Cp ($J.kg^{-1}.K^{-1}$)
Water	0.613	997.1	1.003	4179
Cu	400	8933.0	–	385.0
TiO_2	11.7	4230.0	–	711.75

3.1 Validation of Results

The solution has been validated by comparing in Table 2, drag coefficient, angle of separation and length of reattachment for $Re = 40$, which is the largest value in the range considered for simulation. Values obtained in current simulation are found to match closely with data published in literature.

3.2 Reattachment length

The reattachment length is measured from the downstream side of the cylinder to the point where the velocity changes sign from negative to positive. The comparison between the ratio of the wake length to the cylinder's diameter L/D *vs.* Reynolds number for the solid volume fractions is shown in Figure 2. As shown here, the wake length increases with increasing Reynolds number. Also the wake length increases with increasing solid volume fraction because the flow separation happens earlier in nanofluid comparing with clear fluid. In nanofluid, the separation point moves towards upstream by increasing the solid volume fraction.

Flow separation occurs when the streamlines no longer remain stick to the body and causes wakes near the surface. Angular position of separation point is a function of Reynolds number. Fig. 3 shows the relationship of α_s with Re, it is evident that the point of separation travels upstream with increasing Re.

Table 2 – Validation of present work results with literature values for Re = 40

	Authors	C_D	α_s	L_w/D	a/D	b/D
Exp.	C. and B. [20]	–	126.2	2.13	0.73	0.59
	R. G. et al [10]	1.49	126.4	2.24	0.71	0.59
	L. and F. [14]	1.54	126.4	2.28	0.72	0.60
Numeric	Fornb. [11]	1.50	124.4	2.24	–	–
al study	D. et al. [15]	1.58	127.2	2.35	–	–
	Pres. work	1.50	126.3	2.25	0.71	0.61

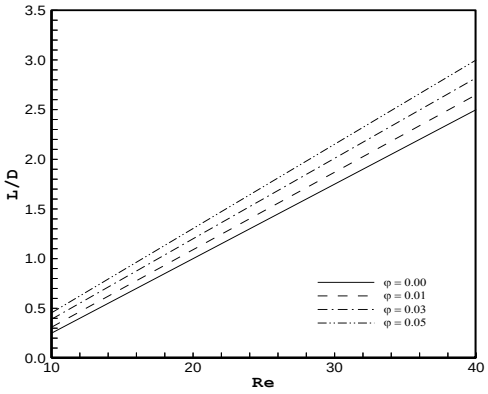

Fig 2 – Variation of wake length with Re at different solid volume fractions φ (Cu)

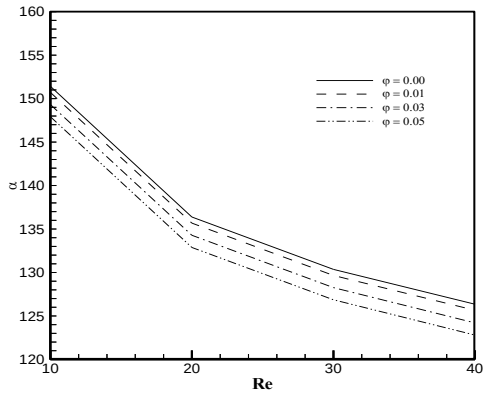

Fig. 3 – Variation of separation angle with Re at different solid volume fractions φ (Cu)

3.3 Effect of Nanoparticle on Augmentation in Heat Transfer

In this section, we investigate the effect of nanoparticle volume fraction on heat transfer performance of nanofluid. The quantification of heat transfer is characterized by local and average Nusselt number. For a nanofluid, the Nusselt number is a function of various factors such as heat capacitance and thermal conductivity of both the base fluid and the nanoparticles, the volume fraction of suspended particles, the viscosity of the nanofluid and the wake structur.

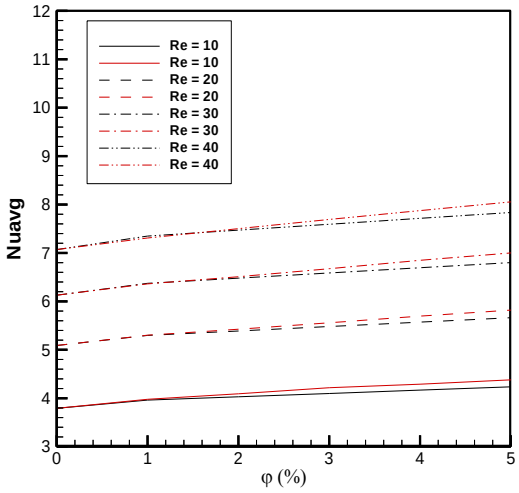

Fig. 4 – Variation of mean Nusselt numbers with volume fraction for different nano-particles (Cu and TiO_2)

The local Nusselt number of the nanofluid, based on cylinder diameter is defined as:

$$Nu = -\left[\frac{k_{nf}}{k_f}\frac{\partial T}{\partial n}\right]_{along\ the\ cylinder\ surface}$$

Surface averaged Nusselt number of fully developed thermal boundary layer is defined as:

$$Nu_{ave} = \frac{1}{s}\int_s Nuds$$

A comparison between local Nusselt numbers along the cylinder for various solid volume fractions and Reynolds number was show in Fig. 5. It can be seen that Nusselt number increase with increase in solid fraction as well as increase in Reynolds number. However, the reason for increase in the two cases is entirely different.

Variation of average Nusselt number for different values of Reynolds number and solid fraction is shown in Fig. 4. In this figure we shows that increasing in both Reynolds number and solid volume fraction will increase the average Nusselt number. One of the main reasons for this behavior is:

– the motion of nanoparticles that transport heat energy.

– the to micro-convection of fluid surrounding nanoparticles.

Fig. 5 presents the variation of mean Nusselt number with volume fraction using different nanoparticles and different values of Reynolds number.

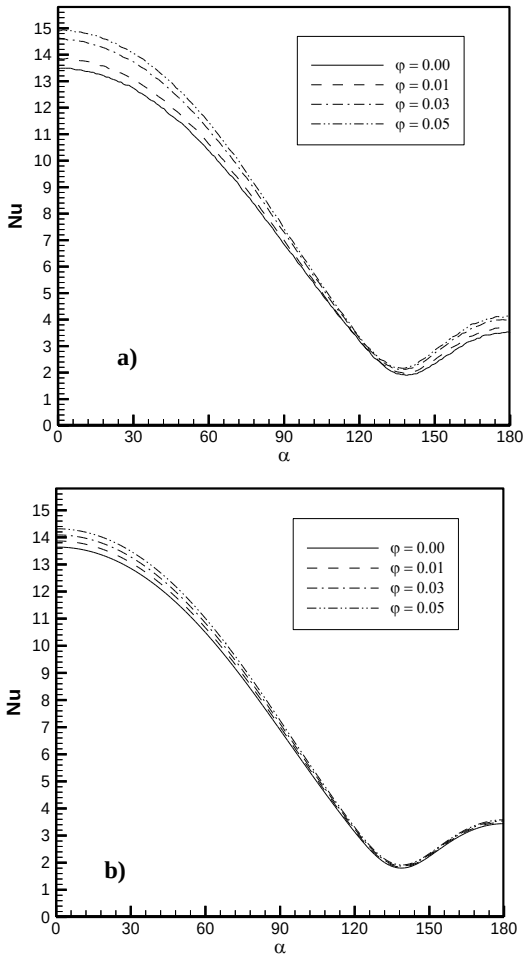

Fig. 5 – Variation of local Nusselt number on cylinder surface with various solid volume fraction φ at Re = 40 Cu (a) and TiO_2 (b)

The figure shows a comparison between Cu-water nanofluid (plotted by red lines) and TiO_2-water nanofluid (plotted by black lines). That the heat transfer with increasing the volume fraction for all Reynolds numbers and nanofluids. The lowest heat transfer was obtained for TiO_2 due to domination of conduction mode of heat transfer since TiO_2 has the lowest value of thermal conductivity compared to Cu.

3.4 Effect of Nanoparticle on Flow Characteristics

Volume fraction of nanoparticles is a key parameter for studying the effect of nanoparticles on flow fields and temperature distributions. Thus, Fig. 6 and Fig. 7 are prepared to present the effect of volume fraction of nanoparticles.

The streamlines, vorticity and isotherm contours around cylinder are compared between clear fluid and nanofluid (φ = 0.05) in Fig. 6 for Reynolds number of 20 and 40. It can be seen that the recirculation length increases as Reynolds number increases in both clear and nanofluid. However, in nanofluid the center of wake is slightly shifted away from the surface of the cylinder comparing with clear fluid. The strength of the vorticity is increased comparison with the nanofluid. For the temperature distribution contours, it can be

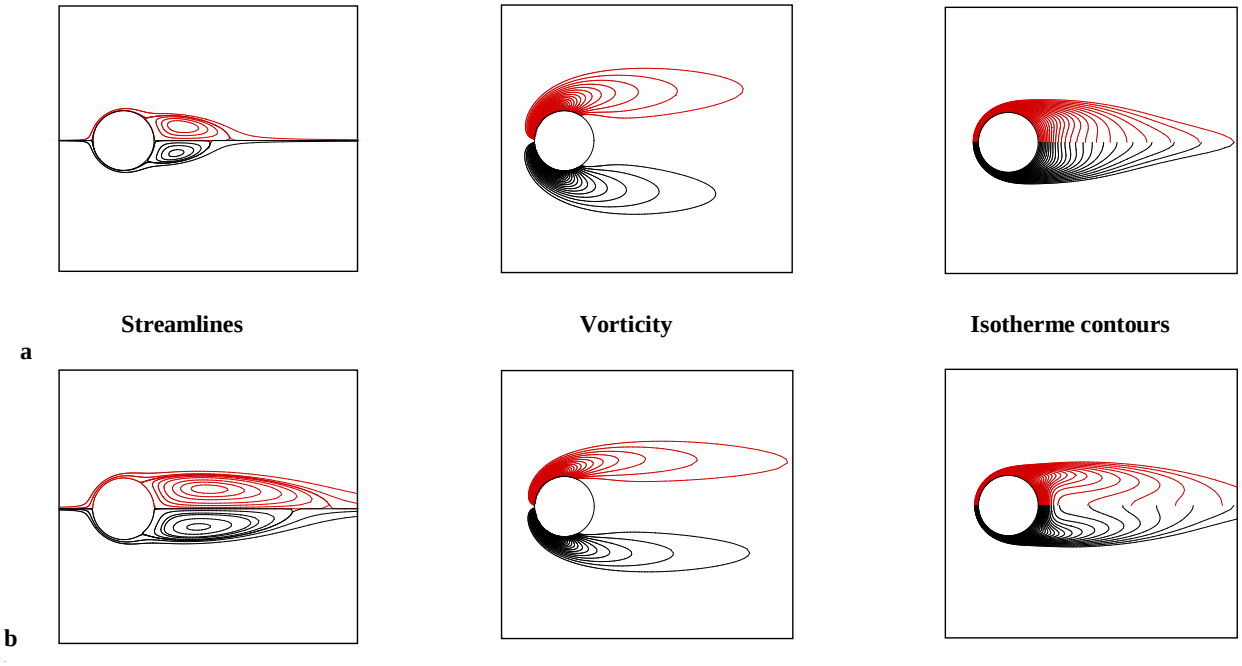

Fig. 6 – The streamlines, vorticity and isotherm contours around the cylinder, (clear fluid (lower half) and water/Cu 5 % (upper half)) at a) Re = 20, b) Re = 40

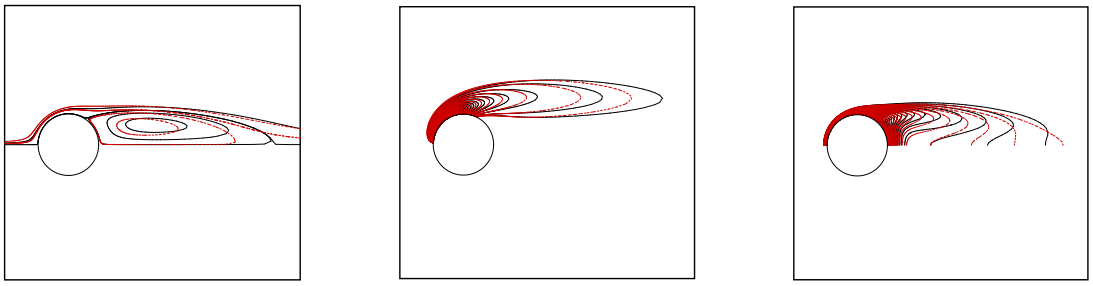

Fig. 7 – The streamlines, vorticity and isotherm contours around the cylinder, (TiO_2-water nanofluid (plotted by red dashed lines) and Cu-water nanofluid (plotted by black solid lines)) at Re = 40

concluded that the temperature contours are steeper in the near-wake region with increasing Reynolds number. This signifies that higher Reynolds number sets a higher temperature gradient. It can also be seen that the nanofluid show higher heat transfer rate from the cylinder than clear fluid.

4. CONCLUSIONS

Steady laminar flow behind a circular cylinder, representing flow around bulff bodies, has been subjected to numerous experimental and computational studies. One of the most prominent flow structure changes takes place in the vicinity of Re < 40. Below this Reynolds number, the flow is characterized by the presence of a symmetric pair of closed separation bubbles. Beyond Re = 40, the flow becomes unsteady and asymmetric, and alternate vortex shedding begins. In this article, the point of investigation was to evaluate the effect of nano-particle on convective heat transfer and flow characteristics. It is observed that the vorticity, pressure coefficient, recirculation length are increased by the addition of nanoparticles into clear fluid. Moreover, the local and mean Nusselt numbers are enhanced due to adding nanoparticles into base fluid.

From this study, we could draw the following conclusions:

• The presence of nanoparticle in the base fluid enhances the heat transfer rate and temperature profiles.

• For all types of nanofluid that have been considered, copper-water and titania-water, the heat transfer rate increases with increasing nanoparticle volume fraction parameter.

• Copper-water working fluid has the highest heat transfer rate followed by titania-water working fluid.

REFERENCES

1. M.S. Valipour, A.Z. Ghadi, *Int. Commun. Heat Mass Transf.* **38**, 1296 (2011).
2. V. E-Farooji, E. E-Bajestan, H. Niazmand, S. Wongwises, *Int. J. Heat Mass Transf.* **55**, 1475 (2012).
3. M.S. Valipour, R. Masoodi, S. Rashidi, M. Bovand, M. Mirhosseini, *Thermal Sci.* **18**, 1305 (2014).
4. S.J.D. D'Alessio, J.P. Pascal, *Acta Mechanica* **117**, 87 (1996).
5. K. Ogawa, C. Kuroda, I. Inoue, *J. Chem. Eng. Jpn.* **17**, 654 (1984).
6. A.T. Srinivas, R.P. Bharti, R.P. Chhabra, *Ind. Eng. Chem. Res.* **48**, 9735 (2009).
7. S. Sandip, G. Suvankar, D. Amaresh, *Int. J. Heat Mass Transf.* **59**, 433 (2013).
8. A.S. Dalkilic, N. Kayaci, A. Celen, M. Tabatabaei, O. Yildiz, W. Daungthongsuk, S. Wongwises, *Curr. Nanosci.* **8**, 949 (2012).
9. M.S. Valipour, R. Masoodi, S. Rashidi, M. Bovand, M. Mirhosseini, *Thermal Sci.* **18**, 1305 (2014).
10. R. Gautier, D. Biau, E. Lamballais, *Computer. Fluids* **75**, 103 (2013).
11. B. Fornberg, *J. Fluid Mech.* **98**, 819 (1980).
12. V.W. Kaufui, O.D. Leon, *Adv. Mech. Eng.* Article ID 519659 (2010).
13. Robert Taylor, et al., *J. Appl. Phys.* **113**, 011301 (2013).
14. M. Linnick, H. Fasel, *J. Comput. Phys.* **204**, 157 (2005).
15. H. Ding, C. Shu, Q. Cai, *Comput. Fluids* **36**, 786 (2007).
16. Y. Ding, et al., *J. Part. Powder* **25**, 23 (2007).
17. D. Chatterjee, B. Mondal, *Int. J. Heat Mass Transf.* **54**, 5262 (2011).
18. N. Masoumi, et al., *J. Phys. D: Appl. Phys.* **42**, 055501 (2009).
19. A. Sharma, V. Eswaran, *Numer. Heat Transfer A-Appl.* **45**, 247 (2004).
20. M. Coutanceau, R. Bouard, *J. Fluid Mech.* **79**, 231 (1977).